

Photoproduction of top in peripheral heavy ion collisions

Spencer R. Klein¹, Joakim Nystrand¹, and Ramona Vogt^{1,2}

¹*Lawrence Berkeley National Laboratory, Berkeley, CA 94720*

²*Physics Department, University of California, Davis, CA 95616*

Abstract

In relativistic heavy ion collisions, top quarks can be produced by photon-gluon fusion when a photon from the Weizsäcker-Williams virtual photon field of one nucleus interacts with a gluon in the other nucleus. Photoproduction with heavy ions at the Large Hadron Collider (LHC) will be the first accessible non-hadronic top production channel. We calculate the $t\bar{t}$ photoproduction cross sections, pair mass and top quark rapidity distributions in peripheral heavy ion collisions. The cross sections are sensitive to the top quark charge and the large- Q^2 gluon distribution in the nucleus. We find a cross section of 94 pb in calcium-calcium collisions, leading to 190 pairs in a one month (10^6 sec) LHC run. We also find $p\text{Pb}$ and $p\text{Ca}$ cross sections of 5.8 and 3.4 pb respectively, resulting in 6 and 34 $t\bar{t}$ pairs per month.

Due to their large charges, relativistic heavy ions carry strong electromagnetic fields which may be treated as virtual photon fields. In a relativistic ion collider, these fields interact with target nuclei in the opposing beam, resulting in high luminosities for photonuclear interactions. Because of the large Lorentz boosts, high photon-nucleon center of mass energies are reached. Previous studies have considered photoproduction of charm [1] and bottom [2] quarks as well as nuclear breakup [3] and vector meson production [4]. These calculations all considered peripheral collisions, with impact parameter, b , greater than twice the nuclear radius R_A so that the two nuclei do not interact hadronically. Peripheral collisions will be studied experimentally at RHIC [5] and the LHC [6], now under construction at CERN.

Here, we consider the production of top quarks via photon-gluon fusion, paralleling previous calculations of photoproduction in heavy ion collisions [1,2]. In these collisions, a $t\bar{t}$ is produced in the reaction $\gamma(k) + A(P) \rightarrow t(p_1) + \bar{t}(p_2) + X$ where k is the four momentum of the photon emitted from the virtual photon field of the projectile nucleus, P is the four momentum of the interacting nucleon in ion A , and p_1 and p_2 are the four momenta of the produced t and \bar{t} quarks. The photons are almost real, with $|q^2| < (\hbar c/R_A)^2$. The slight virtuality is neglected. On the parton level, the photon-gluon fusion reaction is $\gamma(k) + g(x_2P) \rightarrow t(p_1) + \bar{t}(p_2)$ where x_2 is the fraction of the target momentum carried by the gluon. To lowest order (LO), the $t\bar{t}$ production cross section is [7]

$$s^2 \frac{d^2\sigma}{dt_1 du_1} = \pi\alpha_s(Q^2)\alpha e_t^2 \left(\frac{t_1}{u_1} + \frac{u_1}{t_1} + \frac{4m^2s}{t_1 u_1} \left[1 - \frac{m^2s}{t_1 u_1} \right] \right) \delta(s + t_1 + u_1) \quad (1)$$

where the partonic invariants s , t_1 , and u_1 are defined as $s = (k+x_2P)^2$, $t_1 = (x_2P-p_1)^2 - m^2$, and $u_1 = (k-p_1)^2 - m^2$. In this case, $s = (2\gamma^2 - 1)4kx_2m_p$ where γ the Lorentz boost of a single beam and m_p is the proton mass. Here, $\alpha = e^2/\hbar c$ is the electromagnetic coupling constant, $\alpha_s(Q^2) \approx 0.11$ is the strong coupling constant to one loop evaluated at scale Q^2 , $e_t = 2/3$ is the expected top quark charge, and $m = 175$ GeV is the top quark mass. The large mass of the top quark prevents toponium production, allowing the t and \bar{t} to be treated as free quarks, even near threshold [8]. The hadronic top production cross section is obtained by integrating Eq. (1) over x_2 and k ,

$$S^2 \frac{d^2 \sigma_{\gamma A \rightarrow t \bar{t} X}}{dT_1 dU_1} = 2 \int_{k_{\min}}^{\infty} dk \frac{dN}{dk} \int_0^1 \frac{dx_2}{x_2} g(x_2, Q^2) s^2 \frac{d^2 \sigma}{dt_1 du_1}, \quad (2)$$

where dN/dk is the photon flux and the hadronic invariants are $S = (k+P)^2$, $T_1 = (P-p_1)^2 - m^2$, and $U_1 = (k-p_1)^2 - m^2$. Energy conservation determines $k_{\min} = m^2/(2\gamma^2 - 1)x_2 m_p$. The factor of two in Eq. (2) arises because both nuclei emit photons and thus serve as targets. The incoherence of top production guarantees that there is no interference between the two production sources [9].

We use the MRST LO gluon distribution $xg(x, Q^2)$ [10] evaluated at $Q^2 = m^2 + p_T^2$ where p_T is the transverse momentum of the produced top quark. The MRST LO gluon distribution is considerably softer than older, flat parameterizations like $xg(x) \propto (1-x)^n$ [11] used in earlier photoproduction predictions. Calculations with $n = 5$ result in cross sections 2 – 3 times higher than those with the MRST LO gluon distribution. Shadowing, the modification of the gluon distribution in nuclei, is included via a parameterization based on a fit to data [12]. There are two caveats regarding shadowing. First, the large Q^2 of top production is outside the upper bound of the fit, $Q_{\max}^2 = 10^4 \text{ GeV}^2$. The gluon shadowing continues to evolve beyond this point with changes on the percent level between $Q = 100 \text{ GeV}$ and 800 GeV . Second, the probable impact parameter dependence of the shadowing [13] has been neglected.

The photon flux is given by the Weizsäcker-Williams formulae. The flux is a function of the distance from the nucleus, r ,

$$\frac{d^3 N}{dk d^2 r} = \frac{Z^2 \alpha w^2}{\pi^2 k r^2} \left[K_1^2(w) + \frac{1}{\gamma^2} K_0^2(w) \right], \quad (3)$$

where $w = kr/\gamma$ and $K_0(w)$ and $K_1(w)$ are modified Bessel functions. The photon flux is cut off at an energy determined by the size of the nucleus. In the rest frame of the target nucleus, the cutoff is boosted to $(2\gamma^2 - 1)\hbar c/R_A$, or 500 TeV for lead and 1400 TeV for calcium. The $t\bar{t}$ production cross section, $\gamma p \rightarrow t\bar{t}$ [11], for a photon with the cutoff energy of calcium is a factor of 5.5 times larger than the cross section at the cutoff energy of lead. Thus the difference in the energy cutoffs of lead and calcium is significant.

The total photon flux striking the target nucleus is the integral of Eq. (3) over the transverse area of the target at all impact parameters subject to the constraint that the two nuclei do not interact hadronically [1,4]. The numerical result agrees to within 15% of the analytical result,

$$\frac{dN}{dk} = \frac{2Z^2\alpha}{\pi k} \left[w_R K_0(w_R) K_1(w_R) - \frac{w_R^2}{2} (K_1^2(w_R) - K_0^2(w_R)) \right], \quad (4)$$

the integral of Eq. (3) for $r > 2R_A \approx 2.4A^{1/3}$ where $w_R = 2kR_A/\gamma$. The 15% difference can serve as a conservative estimate of the uncertainty on the photon flux; this can be checked using other photoproduction and two-photon interactions.

Although our $t\bar{t}$ calculation is at leading order, the large mass of the top quark ensures faster convergence of the perturbative expansion than for the lighter charm and bottom quarks where the next-to-leading order corrections lead to factors of 2 – 3 enhancements over the LO cross section. The next-to-leading order $t\bar{t}$ cross sections are only $\approx 40\%$ larger than the LO cross sections in pp interactions [14]. We assume the NLO enhancement to be similar for photoproduction.

We consider top quark production at the LHC by lead and calcium ions. The expected energies and luminosities for Ca+Ca and Pb+Pb collisions are given in Table 1 [15].

The top quark rapidity distribution, obtained from Eq. (2), is shown in Fig. 1 for lead and calcium beams. The calculations assume that the photon is in the field of the nucleus coming from negative rapidity so that $y < 0$ corresponds to $k < x_2 m_p$. Since either nucleus can emit a photon, the total $d\sigma/dy$ is the sum of this curve and its mirror image around $y = 0$. Roughly half the production is within $|y| < 1$, in the acceptance of the central detectors planned for the LHC.

The total cross sections for $t\bar{t}$ pair production with lead and calcium beams are 496 pb and 94 pb. As Table 1 shows, a 10^6 s (one month) heavy ion run at design luminosity will produce 0.5 and 190 pairs respectively. The most significant factor in the rate difference comes from the luminosity, 10^3 times higher for calcium. Because of the large luminosity gain, intermediate mass ions are better for studies of nuclear gluon distributions.

The only previous study of $t\bar{t}$ production via photon-gluon fusion in heavy ion collisions [16], used a very different photon flux. The flux was integrated over all r , including the nuclear interior, modelling the nucleus as a homogeneously charged sphere. This approach is flawed because the photon flux inside the nucleus is poorly defined. Ref. [17] shows that the photon flux varies by orders of magnitude inside the nucleus, depending on the chosen nuclear form factor. More importantly, the calculation is incorrect because the photon flux inside the nucleus is much higher than that outside the nucleus. The authors apply a correction factor of 1/2 but this factor is inappropriately large. Their photon flux (and corresponding cross section) for Pb+Pb collisions is a factor of 10 greater than ours.

Shadowing plays little role in the total cross sections since at $y = 0$ and $p_T = 0$, $\langle x_2 \rangle \approx 0.06$ for lead and 0.05 for calcium. These values are in a region where shadowing effects are small. In addition, at the large Q^2 required for top production, shadowing effects should be further reduced by Q^2 evolution [12]. The uncertainty in the large- Q^2 shadowing is significant since no data are available.

The $t\bar{t}$ pair invariant mass distribution, $d\sigma/dM$, is shown in Fig. 2. The larger photon energy for calcium results in a broader pair mass distribution.

These top quark pairs can be observed via their decays, predominantly $t\bar{t} \rightarrow W^+bW^-\bar{b}$, where the W decays to $\ell\nu$ or $q\bar{q}'$. The major background to these channels is likely to be hadroproduction of top in grazing peripheral collisions with slightly smaller impact parameter. The two reactions can be separated based on charged multiplicity, the presence of rapidity gaps in the collision, and the breakup of the colliding nuclei. The average multiplicity in a pp collision at energies of 2.75 – 3.5 GeV/nucleon is expected to be about 45, higher than the roughly 35 particles expected in a γp collision at typical top-production energies [18]. Charged multiplicity will thus be an effective handle for separating the two channels. The multiplicity should be further reduced in top photoproduction since most of the photon energy will be used to produce the $t\bar{t}$ pair, leaving relatively little debris aside from the $t\bar{t}$ decay products.

Because the photon is colorless, even if the nucleus breaks up, photoproduction events

should also have a rapidity gap between the emitting nucleus and the $t\bar{t}$ system.

Nuclear breakup can be a complication for lead since the probability that the lead nucleus is excited into a giant dipole resonance which decays by emitting one or more neutrons is $\approx 35\% \cdot (b/2R_A)^2$ [19]. However, the excitation probability for calcium beams is very small. To a good approximation, the excitation and the photon-gluon fusion occur independently of each other. Thus the two processes factorize and each can be studied independently [20].

Together, these criteria should be almost 100% effective in rejecting hadronic collisions involving more than single nucleon-single nucleon collisions. For single nucleon-single nucleon interactions, they should still be quite effective.

The photoproduction cross sections are larger than the corresponding $pp \rightarrow t\bar{t}X$ cross sections. At lowest order (LO), with $\sqrt{s} = 5.5$ TeV $\sigma(pp \rightarrow t\bar{t}X) = 41$ pb, 10% of the photoproduction cross section for lead, while for calcium at $\sqrt{s} = 7$ TeV, $\sigma(pp \rightarrow t\bar{t}X) = 80$ pb, 85% of the corresponding photoproduction cross section. Thus, only a moderate hadronic rejection factor is required.

Other backgrounds should be small. Hadronic single or double diffractive production without accompanying hadronic interactions, $AA \rightarrow AA\bar{t}tX$ occurs for only a very small range of impact parameters. It is also suppressed by the $1/M^4$ final-state mass dependence. Any single diffractive production of top will be at larger rapidities than photoproduction which is more central. We have calculated the cross section for two-photon production of $t\bar{t}$ and found it to be negligible. Backgrounds from other photoproduction channels should be significantly smaller than at hadron colliders because $\sigma(\gamma p \rightarrow Q\bar{Q}X)/\sigma(\gamma p \rightarrow X)$ is much larger than $\sigma(pp \rightarrow Q\bar{Q}X)/\sigma(pp \rightarrow X)$ at comparable energies.

The top photoproduction cross sections are also measurable in pA collisions, as may be possible at the LHC [6]. The expected energies and luminosities are given in table II. Because the proton and the ion must have the same magnetic rigidity at the LHC and $Z = A$ for the proton, these collisions are at somewhat higher per nucleon energies than the corresponding AA collisions. The cost is that the center of mass is no longer at rest in the lab.

The pA collisions would allow a measurement of the gluon structure function in free protons. A comparison between pA and AA photoproduction data at the same energy would provide a straightforward measurement of nuclear gluon shadowing at Q^2 values far above those currently available. At the maximum energies, we find pPb and pCa cross sections of 5.8 and 3.4 pb respectively. These cross sections are larger than the corresponding per nucleon cross sections in AA collisions for two reasons. First, the energy is slightly higher. Second, the average photon energy is higher in pA because the single protons can approach the photon emitting nucleus more closely than a proton in the center of another nucleus. The pPb and pCa cross sections are quite similar because the larger boost and smaller radius of calcium partly compensate for the larger Z of lead. We obtain 6 and 34 $t\bar{t}$ pairs respectively in 10^6 s run, as shown in Table 2.

Although the top quarks are produced inside the target nucleus, because of their very high boost with respect to the target, they decay well outside the nucleus. For a standard model top width of $\Gamma_t = 1.5$ GeV [21], in the nuclear rest frame the top quarks typically travel over 100 fm before decaying. Thus the $t\bar{t}$ pair acts as a dipole with separation $\hbar c/m \sim 10^{-3}$ fm, resulting in a small interaction cross section. Therefore, aside from debris from the target nucleon, the target nucleus will be relatively undisturbed, leaving the $t\bar{t}$ pair with relatively few accompanying particles.

In conclusion, top quark pairs will be produced via photon-gluon fusion in heavy ion collisions. Heavy ion photoproduction will be the first accessible non-hadronic production channel for $t\bar{t}$ pairs. A 10^6 s calcium run at the LHC will produce 190 $t\bar{t}$ pairs. Similar pA runs will produce 6 and 34 pairs for lead and calcium beams respectively. The significant production rates and the relatively clean environment will allow for measurements of the top charge and mass. In addition, the gluon distribution of the nucleus can be measured at large Q^2 .

This work was supported in part by the Division of Nuclear Physics of the Office of High Energy and Nuclear Physics of the U. S. Department of Energy under Contract No. DE-AC-03-76SF00098.

REFERENCES

- [1] N. Baron and G. Baur, Phys. Rev. C **48**, 1999 (1993).
- [2] M. Greiner, M. Vidović, C. Hoffman, A. Schäfer and G. Soff, Phys. Rev. C **51**, 911 (1995); Ch. Hoffman, G. Soff, A. Schäfer and W. Greiner, Phys. Lett. **B262**, 210 (1991).
- [3] G. Baur, K. Hencken and D. Trautman, J. Phys. G **24**, 1457 (1998).
- [4] S.R. Klein and J. Nystrand, Phys. Rev. C **60**, 014903 (1999).
- [5] J. Nystrand and S. Klein, nucl-ex/9811007, in *Proc. Workshop on Photon Interactions and the Photon Structure*, eds. G. Jarlskog and T. Sjöstrand, Lund, Sweden, September 1998.
- [6] E. Lippmaa *et al.*, *FELIX: A full acceptance detector at the LHC*, CERN/LHCC 97-45, August, 1997.
- [7] L.M. Jones and H.W. Wyld, Phys. Rev. D **17**, 759 (1978).
- [8] I. Bigi, Y. Dokshitzer, V. Khoze, J. Kühn and P. Zerwas, Phys. Lett. **B181**, 157 (1986).
- [9] S.R. Klein and J. Nystrand, Phys. Rev. Lett. **84**, 2330 (2000).
- [10] A.D. Martin, R.G. Roberts, W.J. Stirling and R.S. Thorne, Eur. Phys. J. **C4**, 463 (1998); Phys. Lett. B **443**, 301 (1998).
- [11] H. Fritzsch and K.H. Streng, Phys. Lett. B **72**, 385 (1978).
- [12] K.J. Eskola, V.J. Kolhinen and P.V. Ruuskanen, Nuc. Phys. **B535**, 351 (1998); K.J. Eskola, V.J. Kolhinen and P.V. Ruuskanen, Eur. Phys. J. **C9**, 61 (1999).
- [13] V. Emel'yanov, A. Khodinov, S.R. Klein and R. Vogt, Phys. Rev. C **61**, 044904 (2000); V. Emel'yanov, A. Khodinov, S.R. Klein and R. Vogt, Phys. Rev. Lett. **81**, 1801 (1998).
- [14] M.L. Mangano, P. Nason, and G. Ridolfi, Nucl. Phys. **B373** (1992) 295.
- [15] D. Brandt, K. Eggert, and A. Morsch, CERN AT/94-95(DI), CERN SL/94-04(AP),

LHC Note 264; N. Ahmad *et al.*, *ALICE Technical Proposal*, CERN/LHCC 95-71, December 1995.

[16] S.M. Schneider, W. Greiner and G. Soff, *Phys. Rev. D* **46**, 2930 (1992).

[17] M. Vidovic, M. Greiner, C. Best and G. Soff, *Phys. Rev. C* **47**, 2308 (1993).

[18] C. Caso *et al.*, *Eur. Phys. J.* **C3**, 1 (1998).

[19] K. Hencken, D. Trautmann and G. Baur, *Z. Phys.* **C68**, 473 (1995).

[20] M.C. Abreu *et al.* (NA50 Collab.), *Phys. Rev. C* **59**, 876 (1999).

[21] M. Mangano and T. Trippe, *Eur. Phys. J.* **C3**, 343 (1998).

TABLES

Ion Species	Beam Energy (per nucleon)	Luminosity ($\text{pb}^{-1}\text{s}^{-1}$)	$\sigma(AA)$ (pb)	Rate (per month)
Calcium	3.50 TeV	2×10^{-6}	94	190
Lead	2.75 TeV	1×10^{-9}	496	0.5

TABLE I. Beam energies per nucleon and luminosities for heavy ion collisions at the LHC. The $t\bar{t}$ production cross sections and rates in a one month (10^6 s) AA run are also given.

Ion Species	Beam Energy (per nucleon)	pA Luminosity ($\text{pb}^{-1}\text{s}^{-1}$)	$\sigma(pA)$ (pb)	Rate (per month)
Calcium	5.0 TeV	10^{-5}	3.4	34
Lead	4.4 TeV	10^{-6}	5.8	6

TABLE II. Beam energies per nucleon and luminosities for pA collisions at the LHC. The $t\bar{t}$ production cross sections and rates in a 10^6 s pA run are also given.

FIGURES

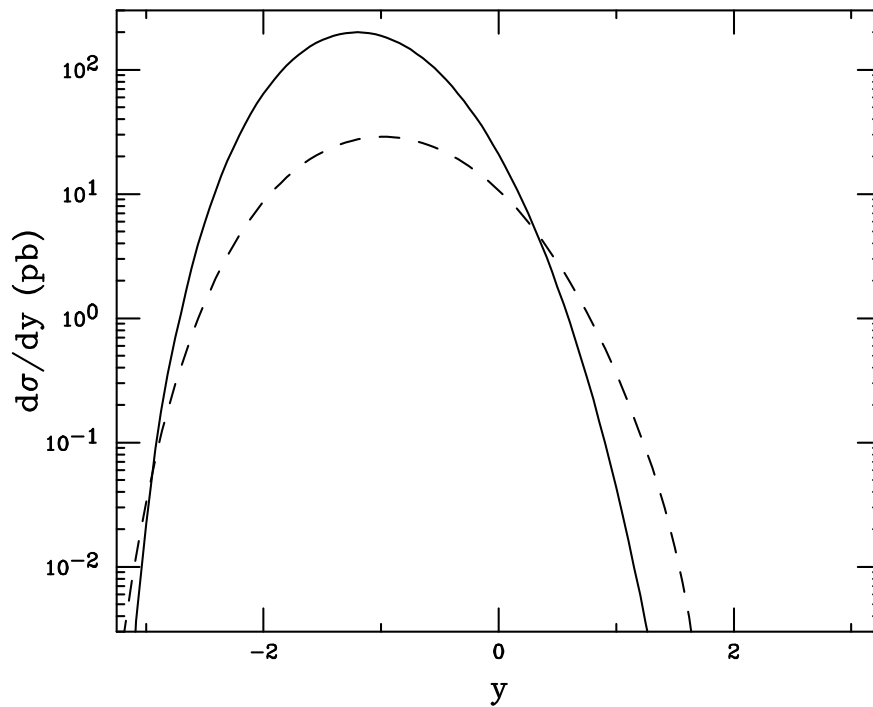


FIG. 1. The top quark rapidity distribution, $d\sigma/dy$, for photoproduced top at the LHC. The solid curve is for Pb+Pb collisions while the dashed curve is for Ca+Ca collisions. In this plot, the photon is emitted by the nucleus with negative rapidity.

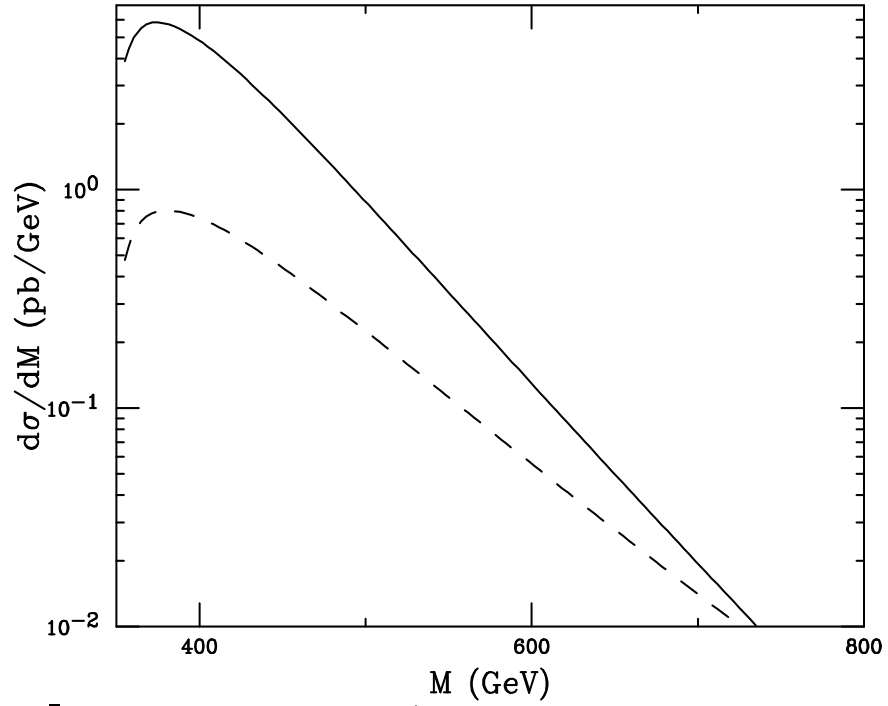


FIG. 2. The $t\bar{t}$ pair mass distribution, $d\sigma/dM$, for photoproduced top at the LHC. The solid curve shows the results for Pb+Pb collisions while the dashed curve is for Ca+Ca collisions.